

Jolanta KRUPA*, Sławomir ZIMOWSKI**

CRACKS DEVELOPMENT FORMED AS A RESULT OF CYCLIC MICRO-IMPACTS ON THE SURFACE OF ANTI-WEAR COATINGS

ROZWÓJ PĘKNIĘĆ POWSTAJĄCYCH W WYNIKU CYKLICZNYCH MIKROUDARÓW NA POWIERZCHNI POWŁOK PRZECIWZUŻYCIOWYCH

Key words:

anti-wear coatings, fatigue, micro-impact.

Abstract:

Fatigue tests are commonly used to define the mechanical properties of materials intended for responsible components operating in various conditions. The fatigue strength of monolithic materials is most often determined during bending, tensile, compression, or torsion tests. The growing area of thin, hard coatings application forced the researchers to extend the fatigue tests to the coating-substrate systems. Since the behaviour of complex, modern materials are not subject to general rules, it is necessary to conduct investigation and analyses and generalise the results of these tests for given groups of materials. In this article, micro-impact fatigue tests were performed to analyse the behaviour of single- and double-layer chromium and chromium nitride coatings. The microhardness and elastic modulus obtained by an indentation method were used to determine the influence of mechanical properties of the coatings on their fatigue wear. After the fatigue tests, the deformation of the coating/substrate system was examined, taking into account the geometry of the craters, and the forms of coating wear caused mainly by cracking were analysed.

Słowa kluczowe:

powłoki przeciwzużyciowe, zmęczenie, mikrouderzenie.

Streszczenie:

Badania zmęczeniowe są powszechnie stosowane do określenia właściwości mechanicznych materiałów przeznaczonych na odpowiedzialne elementy pracujące w różnych warunkach. Wytrzymałość zmęczeniowa materiałów monolitycznych wyznaczana jest najczęściej podczas testów zginania, rozciągania, ściskania lub skręcania. Zwiększenie obszarów zastosowania cienkich, twardych powłok wymusiło na badaczach rozszerzenie testów zmęczeniowych na układy powłoka–podłoże. Ponieważ zachowanie złożonych, nowoczesnych materiałów nie podlega znanym regułom, konieczne jest prowadzenie badań i analiz oraz dążenie do uogólnienia wyników tych badań dla danych grup materiałów. W artykule przeprowadzono mikroudarowe badania zmęczeniowe w celu analizy zachowania przeciwzużyciowych jedno- i dwuwarstwowych powłok chromu i azotku chromu. Przeprowadzone pomiary mikrotwardości i modułu sprężystości metodą indentacyjną pozwoliły na określenie wpływu właściwości mechanicznych powłok na ich zużycie zmęczeniowe. Po testach zmęczeniowych zbadano odkształcenie układu powłoka/podłoże ze względu na geometrię kraterów oraz dokonano analizy form zużycia powłok, którego główną przyczyną było pękanie.

INTRODUCTION

Increased interest in anti-wear coatings in many industrial branches resulted in the development of their manufacturing technologies and methods of testing their properties. The coatings with a complex structure and special applications require

an appropriate, specific method of testing their properties. It allows us to select suitable materials for the chosen purpose. One of the developing methods of examining coatings is a micro-impact test based on cyclic surface fatigue. This technique permits the examination of the coatings as a micro-impact test based on cyclic surface fatigue [L. 1]

* ORCID: 0000-0003-2417-1771. AGH University of Science and Technology, Faculty of Mechanical Engineering and Robotics, A. Mickiewicza 30 Ave., 30-059 Krakow, Poland.

** ORCID: 0000-0002-7348-8751. AGH University of Science and Technology, Faculty of Mechanical Engineering and Robotics, A. Mickiewicza 30 Ave., 30-059 Krakow, Poland.

and was used as a basis in the research. We have investigated the behaviour of single- and double-layer coating systems deposited on ferrite steel. The tests were carried out on the Impact Tester device available at the Laboratory of Tribology of the AGH in Kraków.

FATIGUE TESTS

Dynamic development of material engineering forced scientists to establish unified measure methods of mechanical properties of new materials. Static tensile, compression, bending, and torsion tests are well known and normalised for monolithic materials, the same as fatigue strength tests. The development of coating-substrate systems brought about a change of approach to the properties investigation of such materials. Despite many studies on coatings and their behaviour under static and dynamic loads, there is still no standardisation of these tests.

Nevertheless, in fatigue strength investigation of the coatings, different loading conditions are applied to induce fatigue stress in the coating conducted to fatigue failure. McGrann et al. proposed examining the fatigue life of HVOF (high velocity oxy-fuel) sprayed tungsten carbide (WC) coating using constant deflection bend testing. The stress at the interface between the coating and the substrate was determined from the strain recorded from the strain gauge attached to the bottom of the specimen. An analysis based on the bending of a beam made of two materials was used to calculate the stress in the substrate at the coating/substrate interface [L. 2]. The results of this research as average coating residual stress levels, through-thickness residual stress distributions, fatigue cycles to crack initiation, fatigue cycles to failure, and trend of average coating residual stress level and fatigue life were used to describe the fatigue behaviour of WC coating [L. 3].

Yan et al. investigated torsional strength in both static and fatigue conditions to correlate the measurements. The substrate used was a cylindrical Ti-6Al-4V with hydroxyapatite coating, and the tests were conducted with fixed torque amplitude and frequency. The researchers provided no evident difference between the tensional and torsional tests' results. However, the torsional fatigue strength occurred to be about 35% lower than the static shear strength due to accumulative damage regardless of the coating thickness [L. 4].

The wear behaviour of CrAlN and TiN coatings deposited on TC4 (titanium alloy) was examined with a low-stress tension-tension fatigue test by Bai et al. The researchers studied the effects of fatigue crack initiation and propagation. During elongation, hard coatings have prevented the substrate from plastic deformation and kept its properties even after failure (cracking). Though, due to the poor plastic deformation capacity of the coating, the cracks appeared in the early stage of the fatigue test and propagated quickly to the interface. High-stress concentration increased the effective stress applied to the substrate material under the coating cracks. The findings and measurements showed that with strong adhesion and similar coatings' mechanical properties, the fatigue life of substrate TC4 depends on the coating thickness [L. 5].

Piekoszewski et al. noticed the problem of analysing anti-wear coatings during frictional surface fatigue tests. Covering the substrate with any coating changes the chemical composition and internal strain, changes the physical structure of the surface, and as a result, changes in the influence between the specimen and counter element [L. 6]. Therefore, analysing the friction phenomenon on the substrate-coating system cannot be done the same as on monolithic materials.

However, despite the available test methods and obtained results, research groups have focused on the necessity of wider identification of coatings behaviour in concentrated contact with cyclic fatigue loading. In order to investigate the behaviour of the coatings; it is necessary to provide fatigue tests of multiple impacts with a spherical indenter. Micro-impact tests consist of repeated surface loading in point contact and generating highly concentrated stresses in this area. These tests simulate the conditions that occurred during machining operations, e.g., in cutting tools or forging dies and allow the examination of surface fatigue failure. As Bouzakis et al. mentioned, there is a need to examine whether the coating failure is cohesive or adhesive. The number of impacts which caused coating failure correlated with the applied load gave fundamental information about the coating's durability [L. 7].

The quasi-static and dynamic tests are conducted to correspond the impact forces with the strain rate effect and indicate the failure character. Beake et al. focus on the important relationships of hardness, ductility and wear resistance of hard

coatings, which can be achieved through micro-nano-impact tests [L. 1].

During the repeated impacts of the coating surface with a ball, local deflection of the coating-substrate system and interfacial stress occurs. The variability of the stress leads to the destruction of the coating, which makes it possible to test the adhesive strength of the coating, identify the forms of damage and determine the causes of their occurrence. The impact test methods mentioned above are carried out to determine the fatigue strength of coatings and collect the data supporting the standardisation of these tests, especially for single and multilayer coatings investigations. For this reason, the definition of many variables and their mutual relations are required, but it will make it possible to compare the test results obtained in other laboratories.

This article focuses on investigating fatigue wear of CrN and Cr/CrN coatings under low-cycle micro-impacts. The test results and their analysis will be used in the future to systematise the measurable value of the micro-impact fatigue strength.

EXPERIMENTAL

Materials

Three specimens of chromium (Cr), chromium nitride (CrN) and a bilayer of chromium/chromium nitride (Cr/CrN) coatings were selected for the investigation. The coatings with the same thickness of 1 μm were deposited on ferritic steel by the pulsed laser deposition (PLD) technique. The steel substrates were prepared in the form of plates with dimensions of 20×20 mm and a thickness of 1.5 mm with a one-sided polished surface. Before the coating's deposition, the substrates were cleaned in acetone and ethanol, and then their surfaces were activated in the Ar + O₂ plasma at the pressure of 10⁻² Pa. A high purity target of 99.9 % Cr was used in the ablation process with a pulsed Nd:YAG laser system. The chromium layers were deposited in an argon atmosphere (99.99% Ar) and chromium nitride in a nitrogen atmosphere (99.99% N₂). The outer layer was chromium nitride in the Cr/CrN coating.

Mechanical properties and micro-impact testing

Mechanical properties of the coating-substrate system, such as hardness and modulus of elasticity,

were determined by an instrumental indentation technique using Micro-Combi-Tester (MCT) made by CSEM Instruments Switzerland. The tests were performed using a Vickers diamond indenter under a load of 10 mN. The loading and unloading rate was 20 mN/min and the time of maintaining the maximum load was 5 s. Each of the three specimens was tested at least six times with the same load.

The micro-impact tests have been carried out on Impact Tester [L. 8], which is available in the Laboratory of Tribology and Surface Engineering, AGH UST. The impact tests used ball-shaped alumina (Al₂O₃) indenter of 1 mm in diameter. All specimens were subjected to 1, 5, 10, 25, 50, 100 and 500 load impacts with constant load. The load value has been set to enable the measurement of the geometrical dimensions of the craters that occurred at given cycles. The tests were repeated three times for each specimen with the same number of impacts. The impact tests parameters were equal in all experiments, and they are listed below:

- type of tests: dynamical,
- load of indenter: 4 N,
- frequency: 4 Hz,
- force signal: sinusoidal.

The surface of the tested specimens was examined with Profilm 3D contactless profilometer (Filmetrics Company, USA). The measurements allowed us to observe the geometrical properties of the craters formed during the impact tests. The cross-section area, depth, diameter, volume and apparent contact area of each crater were determined as shown in Fig. 1 and Fig. 2. These measurements provided detailed data for the wear analysis of the coating-substrate system.

RESULTS

The first step in analysing the coatings was to determine the mechanical properties by measuring all specimens' indentation hardness and elastic modulus. Tables 1, 2 and 3 present the calculated average value (\bar{x}) and standard deviation (σ) of Vickers hardness (HV), indentation hardness (H_{IT}), and indentation modulus of elasticity (E_{IT}) for each coating.

The three-dimensional mapping of the crater shape was analysed in two directions. Each profilometer measurement was conducted in two planes – XZ and YZ, as shown in Fig. 1, which allowed two independent crater geometry profiles to be obtained. The analysis focused on the

Table 1. Mechanical properties of Cr coating

Tabela 1. Właściwości mechaniczne powłoki Cr

Cr	HV [-]	H_{IT} [GPa]	E_{IT} [GPa]
\bar{x}	1550	16.3	217
σ	± 206	± 2	± 36

Table 2. Mechanical properties of CrN coating

Tabela 2. Właściwości mechaniczne powłoki CrN

CrN	HV [-]	H_{IT} [GPa]	E [GPa]
\bar{x}	1711	18.1	251
σ	± 288	± 3	± 22

Table 3. Mechanical properties of Cr/CrN coating

Tabela 3. Właściwości mechaniczne powłoki Cr/CrN

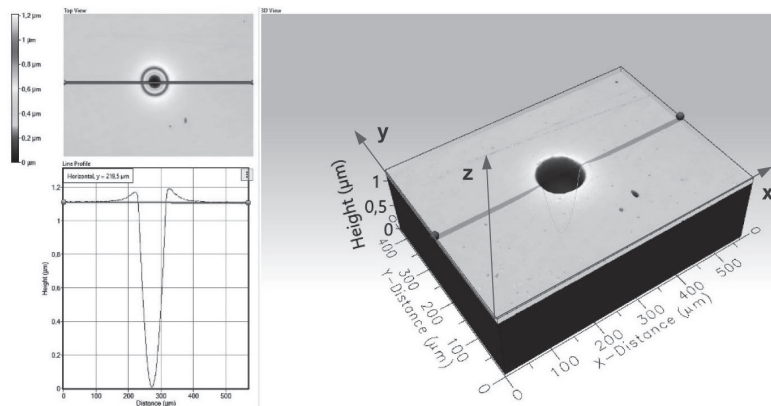
Cr/CrN	HV [-]	H_{IT} [GPa]	E [GPa]
\bar{x}	1620	17.1	228
σ	± 157	± 1.6	± 29

characteristic dimensions of the crater geometry in the coatings marked in **Figure 2**. The plane of reference 0AB was defined individually for each crater, and an apparent contact area was calculated for AB diameter. The average dimensions of the crater geometry for subsequent impact cycles are summarised in **Tables 4–6**.

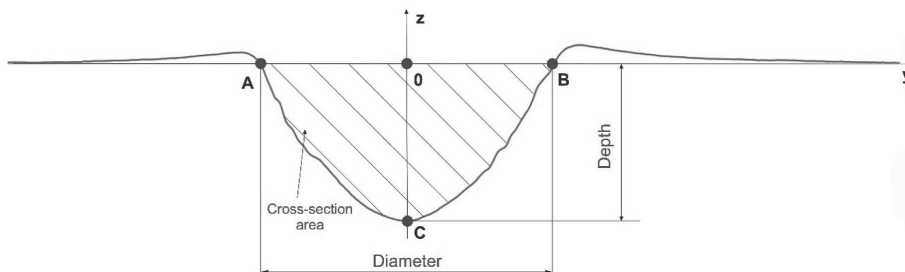
The results of crater geometry measurements in Cr, CrN and Cr/CrN coatings are summarised in **Tables 4–6**. The characteristic dimensions of the craters are presented as average values obtained from three series of tests for each sample. The scatter of the results from the mean value is at a satisfactory level and indicates good repeatability of the tests. In addition, the apparent contact area was calculated from the measured crater diameter in the reference plane. The results of the measurements are also presented graphically in **Figures 3–6**.

In **Figure 7**, the comparison of cross-section geometry of craters in Cr, CrN and Cr/CrN coatings after 500 impact cycles are illustrated.

A microscopic investigation of their surface complemented the study of the characteristic geometric dimensions of the craters to analyse the forms of coating wear. **Table 7** shows the development of coating destruction in the successively selected impact cycles (1, 25, 100, 500 impacts) for each specimen.

**Fig. 1. Graphical representation of a crater measurement made with an optical profilometer**

Rys. 1. Graficzne przedstawienie pomiaru krateru wykonanego przy użyciu profilometru optycznego

**Fig. 2. Characteristic dimensions marked on the vertical section of the crater in the XZ plane**

Rys. 2. Charakterystyczne wymiary oznaczone na przekroju pionowym krateru w płaszczyźnie XZ

Table 4. Characteristic dimensions of the crater's geometry in the Cr coating

Tabela 4. Charakterystyczne wymiary geometrii kraterów w powłoce Cr

Coating material	Cr	Cross-section area [μm^2]		Diameter [μm]		Depth [μm]		Volume [μm^3]		Apparent contact area [μm^2]
		\bar{x}	σ	\bar{x}	σ	\bar{x}	σ	\bar{x}	σ	
Number of impacts	1	38.3	2.6	74.8	0.1	0.720	0.064	1681	155	4392
	5	42.1	3.7	80.9	4.1	0.794	0.071	1952	175	5137
	10	45.6	0.7	83.4	4.7	0.833	0.014	2078	30	5468
	25	51.2	3.3	86.3	4.5	0.914	0.028	2453	206	5854
	50	53.5	8.1	86.3	2.9	0.944	0.092	2789	614	5853
	100	55.3	9.2	89.4	1.2	0.941	0.116	2830	595	6281
	500	78.3	13.3	98.9	4.0	1.256	0.155	4170	328	7689

Table 5. Characteristic dimensions of the crater's geometry in the CrN coating

Tabela 5. Charakterystyczne wymiary geometrii kraterów w powłoce CrN

Coating material	CrN	Cross-section area [μm^2]		Diameter [μm]		Depth [μm]		Volume [μm^3]		Apparent contact area [μm^2]
		\bar{x}	σ	\bar{x}	σ	\bar{x}	σ	\bar{x}	σ	
Number of impacts	1	34.3	1.1	63.8	3.8	0.6675	0.082	1512	231	3194
	5	37.4	5.1	74.3	5.5	0.7141	0.076	1722	236	4331
	10	41.9	4.7	80.0	1.0	0.7824	0.067	1982	230	5028
	25	47.3	4.7	81.9	4.9	0.8342	0.058	2323	249	5273
	50	56.4	8.4	88.4	4.2	0.9544	0.100	2907	493	6140
	100	62.9	10.8	91.4	4.3	1.0299	0.113	3346	646	6558
	500	72.8	8.0	94.5	1.9	1.1645	0.055	4090	254	7012

Table 6. Characteristic dimensions of the crater's geometry in the Cr/CrN coating

Tabela 6. Charakterystyczne wymiary geometrii kraterów w powłoce Cr/CrN

Coating material	Cr/CrN	Cross-section area [μm^2]		Diameter [μm]		Depth [μm]		Volume [μm^3]		Apparent contact area [μm^2]
		\bar{x}	σ	\bar{x}	σ	\bar{x}	σ	\bar{x}	σ	
Number of impacts	1	30.2	4.9	73.8	8.3	0.576	0.083	1336	383	4280
	5	39.4	7.1	75.7	9.0	0.732	0.100	1837	415	4495
	10	44.9	8.3	83.3	3.4	0.800	0.119	2218	493	5445
	25	53.5	5.5	88.2	0.6	0.907	0.081	2692	336	6111
	50	61.4	5.0	91.9	2.1	1.044	0.027	3109	234	6635
	100	62.9	5.2	95.7	1.9	1.047	0.062	3360	285	7192
	500	59.5	3.3	93.7	7.7	1.002	0.005	3175	35	6900

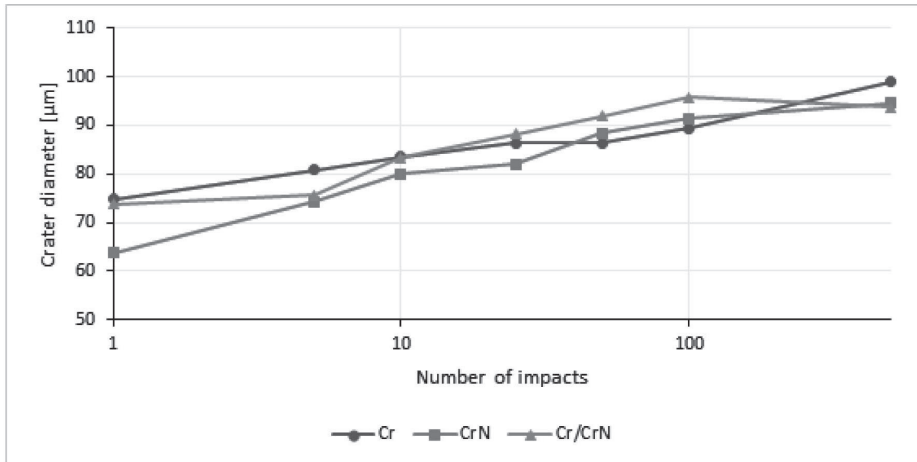


Fig. 3. Diameter of the crater

Rys. 3. Średnica krateru

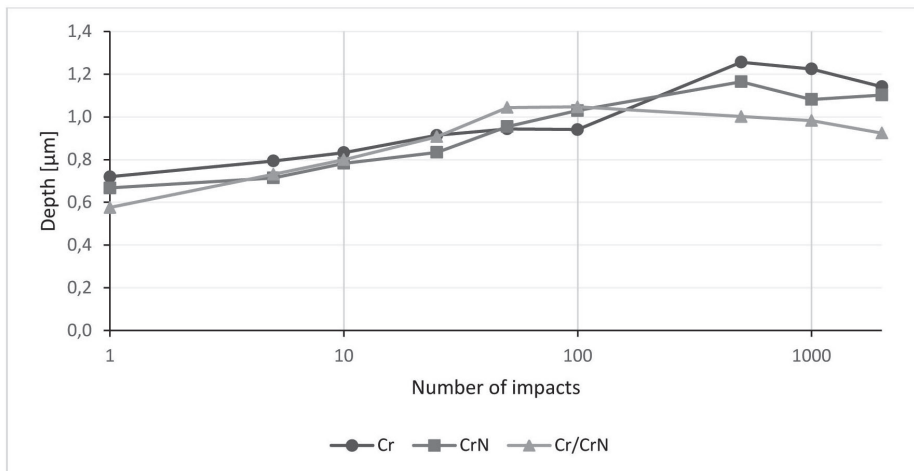


Fig. 4. Depth of the crater

Rys. 4. Głębokość krateru

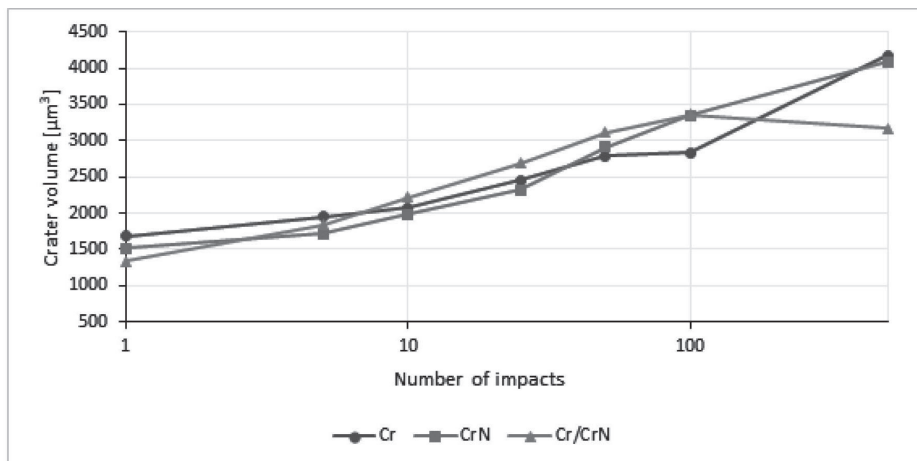
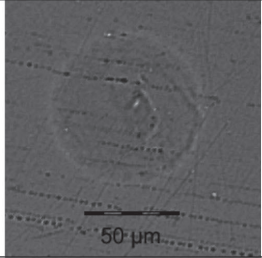
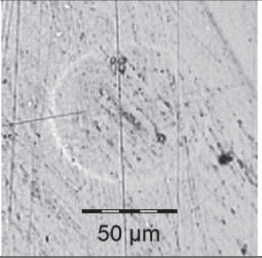
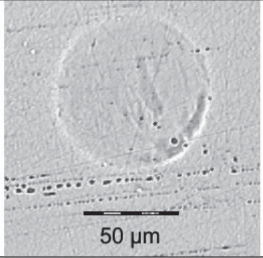
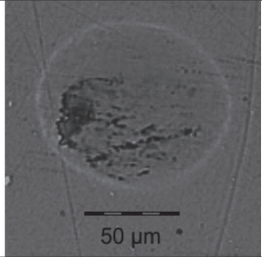
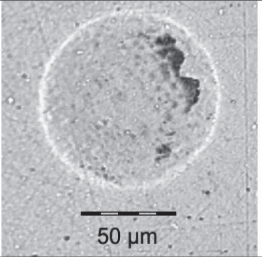
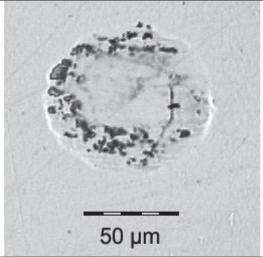
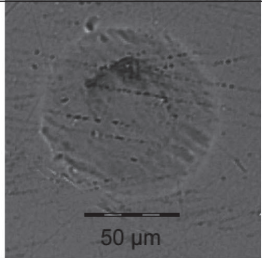
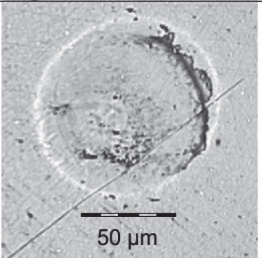
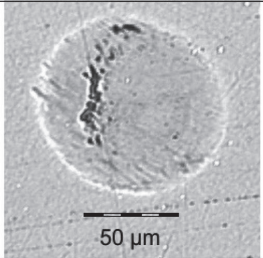
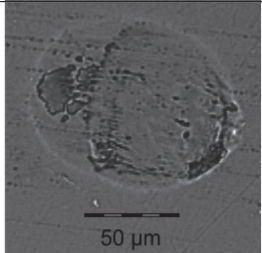
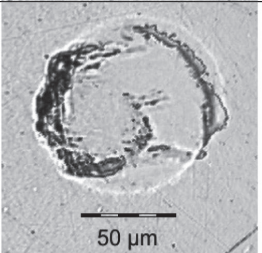
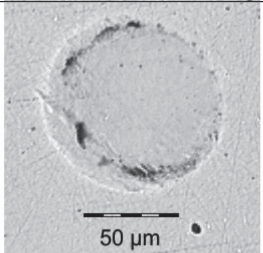


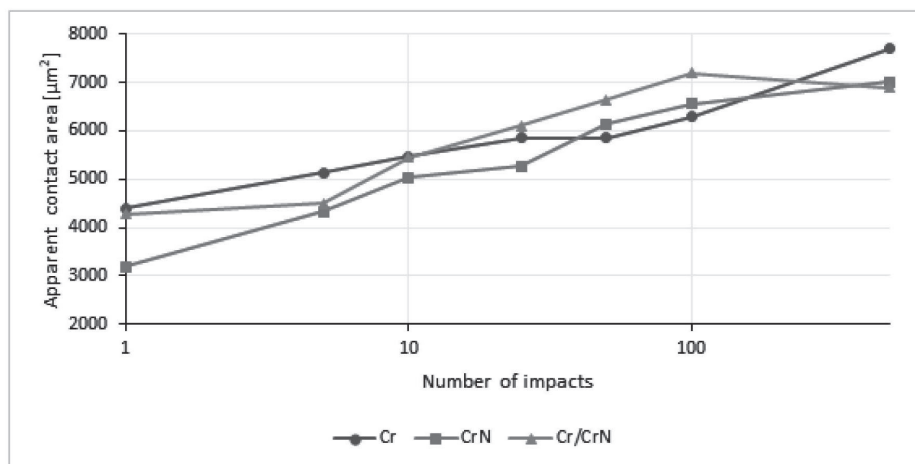
Fig. 5. Volume of the crater

Rys. 5. Objętość krateru

Table 7. Images of the selected craters formed after micro-impacts tests

Tabela 7. Obrazy wybranych kraterów powstałych po zmęczeniowych testach mikrouderzeniowych

Number of impacts	Cr	CrN	Cr/CrN
1			
25			
100			
500			

**Fig. 6. Apparent contact area in the crater**

Rys. 6. Rzut pola kontaktu w kraterze

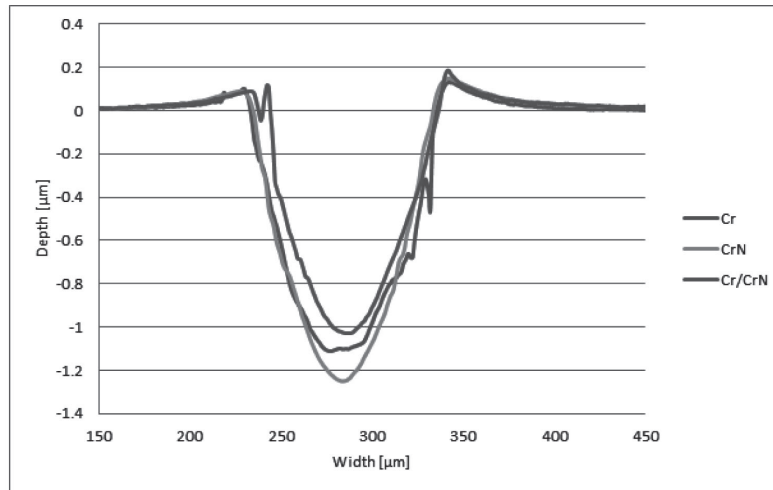


Fig. 7. Cross-section of the craters after 500 impact cycles
 Rys. 7. Przekrój krateru po 500 cyklach uderzeniowych

DISCUSSION

The CrN coating with the highest hardness and stiffness shows the lowest deformation but only with a small number of impacts (**Fig. 1–4**). The first visible coating damage appeared after 25 impacts for the Cr, CrN and Cr/CrN coatings (**Tab. 7**). Even though the ball-shaped indenter was used, the imprints form irregular craters, as shown in **Fig. 7** and **Tab. 7**. In most cases, the failure of coatings in the form of cracks appeared circumferentially but also can be found inside the crater. The coatings were deformed and partly cracked, but none broke off the substrate. The geometrical dimensions of the craters describe the plastic deformation of the coating-substrate system after successive impact cycles. Results show a proportional increase in the geometrical dimensions of the crater with the increase in the number of impacts (**Fig. 3–6**). More than a twofold increase in the crater volume in the range from 1 to 500 impacts at the force of 4 N was found (**Tables 4–6**). Hence, the deformation of the tested coatings was comparable after successive multi-cycle impacts. The relatively high deformability of the coating-substrate system results from the use of the unhardened substrate and the small elastic modulus of the coatings in the range of 220-250 GPa. When analysing the destruction of the coatings, it was found that the fatigue wear resistance depends on their hardness. The CrN coating with the highest hardness underwent significantly greater wear compared

to the Cr coating (**Fig. 7**). This is also confirmed by microscopic observations of the coatings wear at the point of impact, presented in **Tab. 7**. The smallest craters were found in the Cr/CrN coating, with the volume about 28% smaller than the craters in the CrN coating. The crater volume of the hardest CrN coating after 500 impacts was the biggest but only 4% larger compared to the Cr coating with the lowest hardness. The coatings are highly deformed (the crater's depth is up to the coating thickness), but a brittle fracture has not been identified.

SUMMARY

This study discussed the development of the failure of Cr, CrN and Cr/CrN coatings caused by low-cycle micro-impacts. The research methods used in the experimental part allowed the form and size of surface damage to be fully defined, which provided the basis for quantifying coatings wear. The smallest volume of the crater after fatigue micro-impact tests was found in the Cr/CrN bilayer coating. A large contact area favours the absorption of the impact load and better distribution, which reduces the stress concentration. Damage to Cr, CrN and Cr/CrN coatings caused by micro-impacts appeared as the plastic deformation of the coating-substrate system and circumferential cracks observed in the coating. Relatively mild ferritic steel does not provide sufficient resistance against micro-impacts, and hence the coating was forced

into the substrate. In addition, part of the impact energy was consumed in the pile-up of the material around the crater. Nevertheless, any delamination or spalling of the tested coatings was not found, even when the crater depth reached the thickness of the coating. It was found that the initial plastic deformation of the coating-substrate system that occurred during the first few impact cycles is of crucial importance in the development of coating failure. A large contact area favours the absorption of the impact load and a better distribution of pressure, which reduces the stress concentration.

The analysis of coating wear in relation to the crater geometry provides information on the failure development of the coating-substrate system.

ACKNOWLEDGEMENTS

This work was supported by the Polish Ministry of Education and Science under the subvention fund of the Department of Machine Design and Exploitation of AGH-UST (AGH grant number 16.16.130.942).

REFERENCES

1. Beake B.D., Smith J.F.: Nano-impact testing – an effective tool for assessing the resistance of advanced wear-resistant coatings to fatigue failure and delamination. *Surface & Coatings Technology* 2004, 188–189, pp. 594–598.
2. Beer F.P., Johnston E.R., Jr., *Mechanics of Materials* 2012, 2nd ed., pp. 204–207.
3. McGrann R.T.R., Greving D.J., Shadley J.R., Rybicki E.F., Bodger B.E., Somerville D.A.: The Effect of Residual Stress in HVOF Tungsten Carbide Coatings on the Fatigue Life in Bending of Thermal Spray Coated Aluminum. *Journal of Thermal Spray Technology* 1998, 7(4), pp. 546–552.
4. Yan L., Leng Y., Chen J.: Torsional fatigue resistance of plasma sprayed HA coating on Ti-6Al-4V. *Journal of Materials Science: Materials In medicine* 2003, 14, pp. 291–295.
5. Baia Y., Xia Y., Gao K., Yanga H., Panga X., Yangb X., Volinsky A.A.: Brittle coating effects on fatigue cracks behavior in Ti alloys. *International Journal of Fatigue* 2019, 125, pp. 432–439.
6. Piekoszewski W., Szczerek M.: Mechanisms of PVD coated elements surface layer destruction caused by pitting. *Quarterly Tribologia* 2011, 238(4), pp. 229–243.
7. Bouzakis K.-D., Vidakis N., Leyendecker T., Erkens G., Wenke R.: Determination of the fatigue properties of multilayer PVD coatings on various substrates, based on the impact test and its FEM simulation. *Thin Solid Films* 1997, 308–309, pp. 315–322.
8. Krupa J., Wiązania G., Zimowski S., Kot M.: The influence of the multilayer structure of hard coatings on their resistance to micro-impact fatigue wear. *Bimonthly Tribologia* 2020, 290 (2), pp. 37–45.